Progress In Electromagnetics Research Letters, Vol. 13, 139–147, 2010

A DUAL-BAND BANDPASS FILTER HAVING WIDE AND NARROW BANDS SIMULTANEOUSLY USING MULTILAYERED STEPPED IMPEDANCE RESONATORS

M.-H. Weng

Medical Devices and Opto-Electronics Equipment Department
Metal Industries Research & Development Center
3F, No. 88, Luke 5th Road, Lujhu Township, Kaoshiung 82151, Taiwan

S.-K. Liu

Institute of Photonics and Communications
National Kaohsiung University of Applied Sciences
Chien Kung Campus 415 Chien Kung Road, Kaohsiung 807, Taiwan

H.-W. Wu

Department of Computer and Communication
Kun Shan University
No. 949, Dawan Road, Yongkang City, Tainan County 710, Taiwan

C.-H. Hung

Institute of Photonics and Communications
National Kaohsiung University of Applied Sciences
Chien Kung Campus 415 Chien Kung Road, Kaohsiung 807, Taiwan

Abstract—Compact dual-band bandpass filter (BPF) with wide and narrow bands simultaneously is presented. By using the stepped impedance resonators (SIRs) in multilayered structure, the dual-band responses with wide and narrow bands simultaneously can be obtained. The filter has 3-dB fractional bandwidths (FBWs) of 45% and 10% for 2.4 GHz and 5.2 GHz, respectively. The circuit size is compact due to the multilayered structure. Moreover, multi-path propagation inside the multilayered structure generates transmission zeros at each skirt of the passbands for improving the passband selectivity. Measured results of the filter are in good agreement with the full-wave electromagnetic (EM) simulation.

Corresponding author: H.-W. Wu (qqq25q@gmail.com).

1. INTRODUCTION

Bandpass filters (BPFs), especially having a dual-band and characteristic, are popular critical components in multi-service wireless communication and/or wideband communication systems. When designing dual-band BPFs, several schemes can be used, such as cascading coupled-resonators [1], combining with the low- and high-pass circuits [2] and using the coupled-resonators with open or short stubs [3]. Stepped impedance resonator (SIR) is also a well known type to realize dual-band BPF, by shifting its high order resonant modes to desired location [4–7]. However, filters using the above schemes cause a large size since they are fabricated on a single substrate. Moreover, when designing wideband BPFs, the schemes are different from those of dual-band BPFs. For wideband characteristics, the resonators with strong coupling or multi-modes are needed [8, 9]. Therefore, the dual-band BPFs having wide and narrow bands simultaneously challenge designers to obtain the desired coupling coefficients and external quality coefficients, as well as a compact size and a good dual-passband performance. 3-D multilayered structures by low temperature cofired ceramic (LTCC) technologies are well known for very high density circuits [10]. Advantages of the multilayered BPFs also have benefits of strong coupling and cross-coupling effects between the resonators to achieve the desired bandwidth and provide transmission zeros for improving the passband selectivity [11].

In this paper, we present the design of the dual-band BPF with different bandwidths within two passbands by adopting the SIRs in multilayered structure. The design procedure includes the resonant characteristic of SIR, determination of the coupling coefficients and external quality coefficients. The measured results of the filter show a good agreement with the IE3D full-wave simulation [12].

2. DESIGN CONCEPT

Figure 1(a) shows the 3-D view of the multilayered dual-band BPF. The filter mainly consists of four folded SIRs and tapped input/output (I/O) lines connecting with SIR 1 and SIR 4. SIR 2 and SIR 3 are arranged on the 1st substrate, underneath the SIR 1 and SIR 4, as shown in Fig. 1(b). To reduce the circuit size, each SIR is folded. Fig. 2 shows the coupling paths of the typical and proposed coupled-resonators for dual-band BPF.

As shown in Fig. 2(a), the typical coupling structure only provides two coupling paths to introduce one transmission zero between two passbands [9]. However, the proposed coupling structure shown in

Fig. 2(b) could not only save the circuit size, but also provide multi-path propagation from multilayered structure. It is expected that more than two transmission zeros are introduced at each skirt of the passbands to improve the passband selectivity.

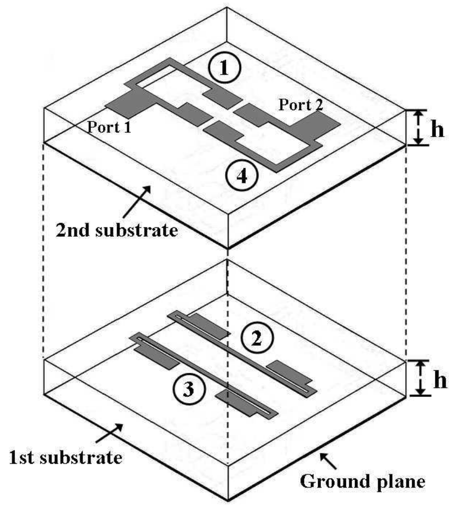

(a)

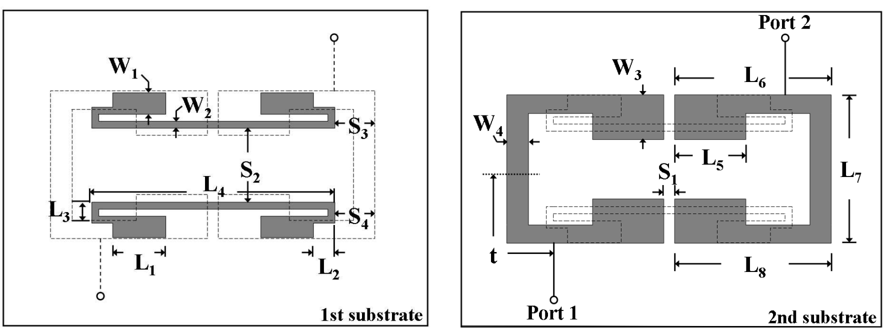

(b)

Figure 1. (a) 3-D view and (b) top view of the dual-band bandpass filter. The two used substrates are Duroid 5880 substrate with a relative dielectric constant $\varepsilon_r = 2.2$, a loss tangent $\tan\delta = 0.0009$, and a thickness $h = 0.787\,\text{mm}$.

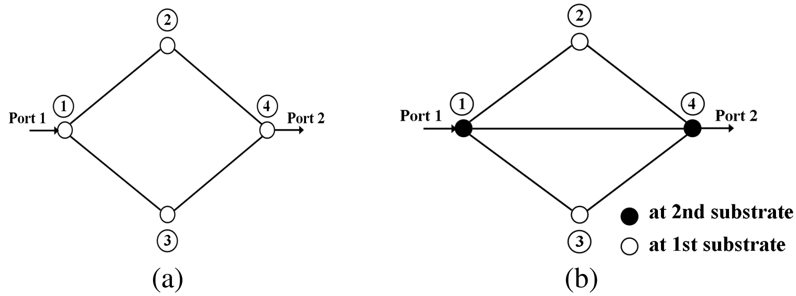

Figure 2. Coupling paths of (a) the typical and (b) the proposed coupled-resonators for dual-band bandpass filter. The node indicates the resonator and solid lines mean the coupling paths between the adjacent resonators.

2.1. Resonant Characteristics of Stepped Impedance Resonator

The impedance ratio $K(= Z_2/Z_1)$ and the length ratio $\alpha = \theta_2/0.5\theta_t$ of the half-wavelength SIR can be used to determine the position of the fundamental resonances (f_0) and the second resonances (f_{s1}) over a wide frequency range. The resonance conditions are determined as follows [7]

$$K \cdot \cot\left(\frac{\alpha\theta_t}{2}\right) = \tan\left(\frac{(1-\alpha)\,\theta_t}{2}\right) \quad \text{for odd mode} \tag{1}$$

$$K \cdot \cot\left(\frac{\alpha\theta_t}{2}\right) = -\cot\left(\frac{(1-\alpha)\,\theta_t}{2}\right) \quad \text{for even mode} \tag{2}$$

Solutions of θ_t are dependent on the choice of K and α. Fig. 3 shows the normalized ratios of f_{s1}/f_0 for the SIR with $K = 0.55, 0.75, 1, 1.25$ and 1.55. For the specification, FBW of 45% at 2.4 GHz and FBW of 10% at 5.2 GHz with the same passband ripple of 0.01 dB are designed. Considering that $f_0 = 2.4$ GHz and $f_{s1} = 5.2$ GHz ($f_{s1}/f_0 = 2.17$) with $K = 0.55$, the length ratio α can be explicitly determined as nearly 0.27 or 0.88. We choose $\alpha = 0.27$ for achieving the miniaturized circuit size of the filter. The design parameters of the SIRs are found to be $\alpha = 0.27$ and $K = 0.55$ with $Z_1 = 110\,\Omega$ and $Z_2 = 60\,\Omega$ in this work.

2.2. Determination of Coupling and Quality Factor

Figure 4 shows the equivalent circuit model of the proposed filter. Frequency independent admittance inverters J_{ij} (i and j denote the

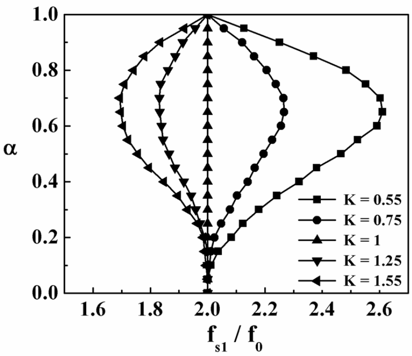

Figure 3. Normalized ratios of the higher order resonant frequencies for the stepped impedance resonator with $K = 0.55, 0.75, 1, 1.25$ and 1.55.

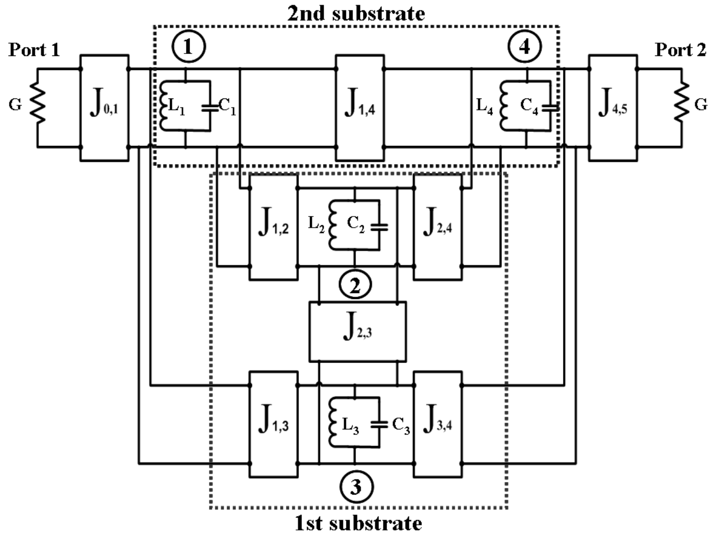

Figure 4. Equivalent circuit model of the multilayered dual-band bandpass filter.

number of SIRs) are used to describe the coupling between two SIRs. The model indicates the multi-path propagation existed in the multilayered structure. For satisfying the required targets, the lumped circuit element values of the prototype lowpass filter are found to be $g_0 = 1$, $g_1 = 0.9491$, $g_2 = 1.3508$, $J_1 = -0.1172$ and $J_2 = 1.0119$ [13]. The coupling matrix M and external quality factors Q_e of the proposed

BPF at two passbands are obtained as follows

$$M^I = \begin{bmatrix} 0 & 0.4 & 0.4 & -0.055 \\ 0.4 & 0 & 0.33 & 0.4 \\ 0.4 & 0.33 & 0 & 0.4 \\ -0.055 & 0.4 & 0.4 & 0 \end{bmatrix}, \quad Q_e^I = 2.11 \tag{3}$$

$$M^{II} = \begin{bmatrix} 0 & 0.088 & 0.088 & -0.012 \\ 0.088 & 0 & 0.075 & 0.088 \\ 0.088 & 0.075 & 0 & 0.088 \\ -0.012 & 0.088 & 0.088 & 0 \end{bmatrix}, \quad Q_e^{II} = 9.49 \tag{4}$$

where $M_{1,4} = \text{FBW}\cdot J_1/g_1$, $M_{2,3} = \text{FBW}\cdot J_2/g_2$, $M_{1,2} = M_{4,2} = M_{1,3} = M_{4,3} = \text{FBW}/(g_1 g_2)^{-0.5}$ and $Q_e = g_0 g_1/FBW$ [13]. The subscript I and II means the first and second passband. The practical coupling coefficient M_{ij} as function of the coupling gap between the SIRs can be determined by

$$M_{ij} = \pm\frac{f_2^2 - f_1^2}{f_2^2 + f_1^2} \tag{5}$$

where f_1 and f_2 indicates the 1st and 2nd operating frequency between two coupling SIRs and subscript i and j indicates the index of SIR, as shown in Fig. 1.

After receiving the initial values of coupling gap between the SIRs, the values are further tuned to satisfy the coupling degree between the adjacent resonators. Noted that the coupling strength between SIR 1

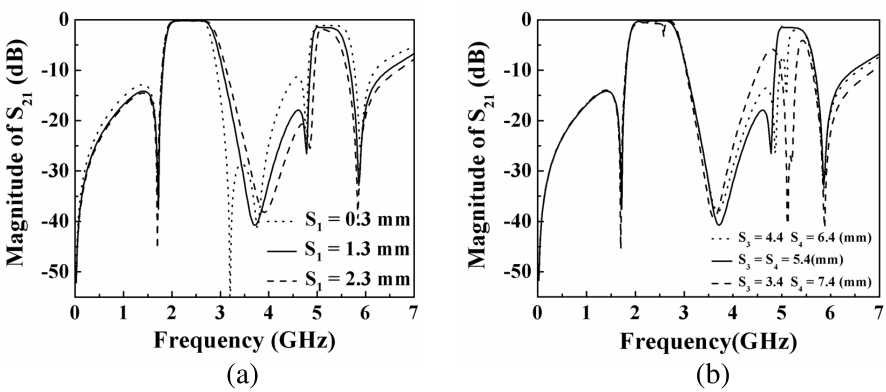

Figure 5. Simulated frequency responses of the multilayered dual-band bandpass filter against (a) the coupling gap S_1 and (b) the position (S_3 and S_4) between SIR 2 and SIR 3. (Other parameters of dimension are fixed for all cases).

and SIR 4 is lower, careful tuning for the coupling gap is necessary to achieve good filter performance. Fig. 5(a) shows the simulated frequency response against the coupling gap S_1 of the filter. It is found that the bandwidth of first passband can be further tuned around 10% by changing the S_1 from 0.3 to 2.3 mm and the good filter response is obtained when $S_1 = 1.3$ mm. Fig. 5(b) shows the simulated frequency response of the filter with different position (S_3 and S_4) between SIR 2 and SIR 3. When $S_3 = S_4$, good inter-coupling from the multilayered structure is achieved to introduce the transmission zeros at each skirt of passbands. To satisfy the external quality factor, the tapped position (t) of the I/O lines is tuned. From the design curve shown in Fig. 6, tapped position $t = 9.3$ mm for Q_e^{II}/Q_e^{I} can be achieved.

3. RESULTS

The designed multilayered dual-band BPF was fabricated and measured by using HP 8510C vector network analyzer (VNA). The circuit size is $32.1 \times 21 = 672\,\text{mm}^2$, approximately $0.38\lambda_g \times 0.25\lambda_g$, where λ_g is the guided wavelength at center frequency of the first passband. Overall circuit size is actually reduced by the multilayered

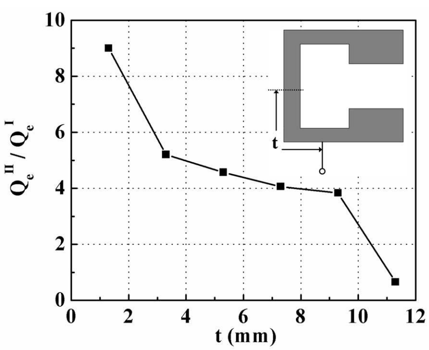

Figure 6. External quality factor Q_e of the multilayered dual-band bandpass filter with the tapped position (t) of the I/O lines.

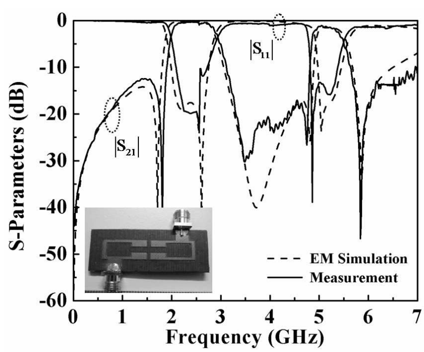

Figure 7. Simulated and measured frequency responses of the multilayered dual-band bandpass filter. $W_1 = 1.6$, $W_2 = 0.6$, $W_3 = 3.2$, $W_4 = 1.2$, $L_1 = 5.4$, $L_2 = 1.9$, $L_3 = 1.5$, $L_4 = 21.7$, $L_5 = 5.4$, $L_6 = 15.7$, $L_7 = 9.8$, $L_8 = 15.7$, $t = 9.3$, $S_1 = 1.3$, $S_2 = 4.4$ and $S_3 = S_4 = 5.4$. All are in mm.

structure. The size is around 30% reduction in comparison of the past literature [11]. Fig. 7 shows the simulated and measured frequency responses. Measured results have $|S_{11}|$ of 20 dB, $|S_{21}|$ of 0.29 dB and FBW of 46% at 2.4 GHz; and $|S_{11}|$ of 15 dB, $|S_{21}|$ of 0.9 dB and FBW of 12% at 5.2 GHz. The filter is four-pole based structure but the six-pole-like frequency response is shown over the frequency range. The multi-path propagation in the multilayered structure introduces several transmission zeros at each skirt of the passbands, actually improving the band selectivity.

4. CONCLUSION

The design of dual-band BPF with much different FBWs has been presented. The proposed filter has FBWs of 46% and 12% at 2.4/5.2 GHz, respectively. By tuning the impedance ratio and length ratio of the SIRs, the dual-band response can be well controlled. Wideband characteristic at single passband can be achieved by the multilayered structure. Multi-path propagation inside the multilayered structure can improve the passbands selectivity. This type of filter is actually suitable for modern mobile wireless communication systems, requiring different FBWs for the two passbands and greatly reduces the circuit size when needing strong coupling by multilayered structure.

REFERENCES

1. Miyake, H., S. Kitazawa, T. Ishizaki, T. Yamada, and Y. Nagatomi, "A miniaturized monolithic dual band filter using ceramic lamination technique for dual mode portable telephones," *IEEE MTT-S Int. Microw. Symp. Dig.*, Vol. 2, 789–792, 1997.
2. Joshi, H. and W. J. Chappell, "Dual-band lumped-element bandpass filter," *IEEE Trans. Microw. Theory Tech.*, Vol. 54, No. 12, 4169–4177, 2006.
3. Tsai, L. C. and C. W. Huse, "Dual-band bandpass filters using equallength coupled-serial-shunted lines and Z-transform techniques," *IEEE Trans. Microw. Theory Tech.*, Vol. 52, 1111–1117, 2004.
4. Lee, C. H., I. C. Wang, and C. I. G. Hsu, "Dual-band balanced BPF using $\lambda/4$ stepped-impedance resonators and folded feed lines," *Journal of Electromagnetic Waves and Applications*, Vol. 23, 2441–2449, 2009.
5. Lee, C. H., C. I. G. Hsu, and Y. C. Chen, "Design of dual-band bandpass filter incorporating tri-section SIRs and CPW SIRs,"

Journal of Electromagnetic Waves and Applications, Vol. 18, 13–18, 2009.

6. Weng, M. H., H. W. Wu, and Y. K. Su, "Compact and low loss dual-band bandpass filter using pseudo-interdigital stepped impedance resonators for WLANs," *IEEE Microw. Wireless Compon. Lett.*, Vol. 17, 187–189, 2007.
7. Chen, C. F., T. Y. Huang, and R. B. Wu, "Design of dual- and triple passband filters using alternately cascaded multiband resonators," *IEEE Trans. Microw. Theory Tech.*, Vol. 54, 3550–3558, 2006.
8. Lin, Y. S., W. C. Ku, C. H. Wang, and C. H. Chen, "Wideband coplanar-waveguide bandpass filters with good stopband rejection," *IEEE Microw. Wireless Compon. Lett.*, Vol. 14, 422–424, 2004.
9. Shanman, H. and J. S. Hong, "Input and output cross-coupled wideband bandpass filter," *IEEE Trans. Microw. Theory Tech.*, Vol. 55, 2562–2568, 2007.
10. Djoumessi, E. E. and K. Wu, "Multilayer dual-mode dual-bandpass filter," *IEEE Microw. Wireless Compon. Lett.*, Vol. 19, 21–23, 2009.
11. Chen, C. C., "Dual-band bandpass filter using coupled resonator pairs," *IEEE Microw. Wireless Compon. Lett.*, Vol. 15, 259–261, 2005.
12. IE3D Simulator, Zeland Software, Inc., Fremont, CA, 1997.
13. Hong, J. S. and M. J. Lancaster, *Microstrip Filters for RF/Microwave Applications*, John & Wiley, New York, 2001.